JOURNAL OF Materials CHEMISTRY

Peroxo sol–gel preparation: photochromic/electrochromic properties of Mo–Ti oxide gels and thin films

Zhongchun Wang,*[a,b] Xingfang Hu[b] and Ulf Helmersson[a]

[a]*Department of Physics and Measurement Technology, Linköping University, SE-581 83 Linköping, Sweden*
[b]*Shanghai Institute of Ceramics, Chinese Academy of Sciences, Shanghai 200050, P. R. China*

Received 20th June 2000, Accepted 21st July 2000
First published as an Advanced Article on the web 5th September 2000

Metallic Mo powder and $Ti(OBu^n)_4$ were separately dissolved in H_2O_2 solution and the solutions obtained mixed in different Mo/Ti atomic ratios to prepare precursor solutions. Fresh gels obtained from the precursor solutions with >40% Mo became blue upon exposure to ambient light. X-Ray photoelectron spectroscopy (XPS) was used to examine the chemical states and compositions of the resultant blue-tinged xerogel powders. Based on the XPS results, it is proposed that TiO_2 particles and surface species, including adsorbed water and organic residue, all contribute to the photochromic effect of MoO_3. Mo–Ti oxide films were spin-coated on ITO-coated glass substrates using a precursor solution containing 70% Mo. The cycling behaviours of the films annealed at 150 °C for 1 h were studied using cyclic voltammetry (CV) in propylene carbonate solution containing 1 mol L^{-1} $LiClO_4$. The electrochromic properties of the films upon lithium intercalation were investigated by *in situ* monochromatic transmittance measurements during the CV process, as well as *ex situ* in the UV/Vis region. The Mo–Ti oxide films were found to possess excellent electrochromic properties upon Li^+ ion insertion/extraction.

1 Introduction

Electrochromic oxide films, such as WO_3 and some other transition metal oxides, are reversibly coloured by the simultaneous injection of small ions, *e.g.* H^+ or Li^+, and an equal number of electrons (from an externally applied source), as shown in reaction (1)

$$MO_n + xA^+ + xe^- \Leftrightarrow A_xMO_n \quad (1)$$

where M is a transition metal and A^+ the small ion.

Applications for electrochromic materials are numerous; they find utility in industrial products such as architectural glazings,[1] ophthalmics, instrumentation devices and displays.[2]

Apart from WO_3, Mo and Ti oxides are also well-known electrochromic materials. Mo oxide[3,4] has a high charge capacity but a low stability against degradation. Ti oxide,[3,5] on the other hand, shows high electrochemical stability but has a high colouring potential, which limits the choice of suitable counter electrodes for electrochromic devices. By adding Ti oxide to Mo oxide, the electrochemical stability is improved,[6] the colouring potential increased and the colouration efficiency decreased.[7] Mo–Ti oxides also exhibit a more neutral colour upon ion insertion than the pure constituents. The broadening of the absorption peak causing the neutral colour for mixed electrochromic materials is also known for other binary oxides[8,9] and is an advantage for several practical applications.

It is well known that metallic Mo, W and Nb react readily with hydrogen peroxide to form peroxo polymetallate acids. The same applies for Ti metal, but with an undesirably low reaction rate if ammonia is not added. Recently, we developed an easy way to prepare peroxo polytitanic acid precursor solution to fabricate TiO_2 thin films by the spin-coating technique, in which we directly react $Ti(OBu^n)_4$ with H_2O_2.[10] The moisture insensitivity of the precursor solutions is notably different from those conventionally used in the sol–gel method, and renders this peroxo sol–gel route very attractive. Prompted by these results, we have used this novel method to prepare Mo–Ti mixed oxide gels and thin films. We report here the preparation of the precursor solutions, photo-colouration of the gel and electrochromic properties of the thin films.

2 Experimental

Precursor solution preparation and thin film fabrication

The procedures for the preparation of the peroxo polytitanic (PPT) acid solutions are detailed in our previous work.[10] Concisely, titanium butoxide, $Ti(OBu^n)_4$, was slowly added to ice-cooled 15% H_2O_2 solution under vigorous agitation. A red solution was immediately obtained, indicating the formation of a Ti–H_2O_2 complex, which is quite unstable and decomposed readily giving off bubbles. The decomposition reaction is self-accelerating. After a while, a vigorous exothermic reaction took place, giving off a large amount of heat and gases containing water, oxygen and organics. The PPT acid gel was then obtained. This can be easily dissolved to form a solution with some dilute H_2O_2 solution.

On the other hand, peroxo polymolybdate (PPM) acid solution was prepared following the method adopted in the literature.[11] Metallic molybdenum powder was added slowly to an ice-cooled beaker containing 15% H_2O_2 solution with stirring, and a red–brown solution was obtained. Various amounts of the above two solutions were combined to afford mixtures with different Mo/Ti atomic ratios. After removing very small amounts of insoluble impurities by filtration, the Mo–Ti mixed oxide precursor solutions were prepared.

The viscosity of the mixed oxide precursor solutions was adjusted by evaporating some water under reduced pressure. The pure Ti solution became a gel easily, while the greater the amount of Mo solution added, the longer the gelation time for the mixed solutions became. After adjustment of the viscosities to a suitable level, the precursor solutions were spin-coated onto indium tin oxide (ITO) conductive glass substrates (with a sheet resistance of 11 Ω $\square^{-1}$). After heat treatment in an oven at 150 °C for 1 h, homogeneous transparent thin films were obtained. The films studied in this work were made by one spin

 DOI: 10.1039/b004933f

and were 120 nm in thickness, as measured by a Talystep profilometer.

Measurements

Diffuse reflection spectra of the gel and powder were measured using a CARY 2390 spectrophotometer with an integrating sphere. Both the diffuse and specular components of the radiation reflected from the sample were measured.

The thermal properties of the mixed oxide precursor xerogels were investigated by TG-DTA carried out on TA Instruments TGA 2050 and DSC 2910 machines at a heating rate of 10 °C min^{-1} in air.

The chemical states and compositions of the mixed oxide powders were analyzed by X-ray photoelectron spectroscopy (XPS) using a VG Microlab 310F system. XPS was carried out using a non-monochromated Mg-Kα (1253.6 eV) X-ray source, a hemispherical electron energy analyzer and a take-off angle of 90°. All the regional XPS spectra were calibrated with the binding energy of the adventitious C 1s peak (284.6 eV), and a Shirley-type background was subtracted.

Cyclic voltammetry (CV) was carried out on Mo–Ti oxide films immersed in an electrolyte of 1 M $LiClO_4$ in propylene carbonate (PC). A standard three-electrode arrangement was adopted, with Pt as the counter electrode, and a saturated calomel electrode (SCE) as the reference electrode. Constant and sweep potentials were provided by a potentiostat and a function generator, respectively. The optical properties of the thin films were measured by a grating spectrophotometer. All data were taken under a dry atmosphere in a glove box with a data acquisition system interfaced to a personal computer.

3 Results and discussion

Thermal properties of the Mo–Ti oxide gel

TG and DTA curves for the mixed oxide precursor xerogel with 70% Mo are shown in Fig. 1. On the DTA curve, a large endothermic peak appears at 110 °C due to the loss of physically or chemically adsorbed water and organic residues. The hump at 330 °C on the DTA curve could be ascribed to the decomposition of the peroxo group, whereas the peak at 600 °C might be due to crystallisation of TiO_2 to the anatase phase. This crystallisation temperature is much higher than that observed for pure TiO_2 gel in our previous work.[10] Obviously, MoO_3 greatly hinders the crystallisation of TiO_2. The large endothermic peak on the DTA curve, and the corresponding large weight loss on the TG curve, at 800 °C are due to the sublimation of MoO_3.

Ambient light photo-colouration of the Mo–Ti oxide gels

The as-prepared Mo–Ti mixed oxide precursor solutions looked yellowish to the naked eye. However, fresh gels

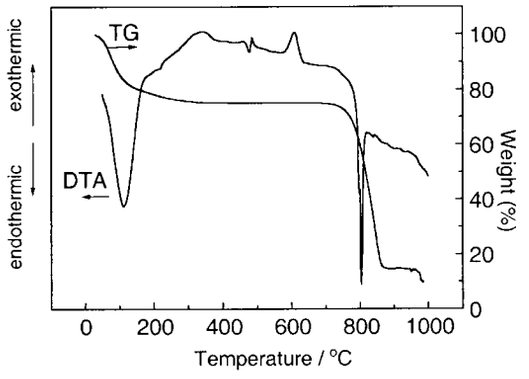

Fig. 1 TG-DTA curves for the as-dried Mo–Ti oxide gel containing 70% Mo.

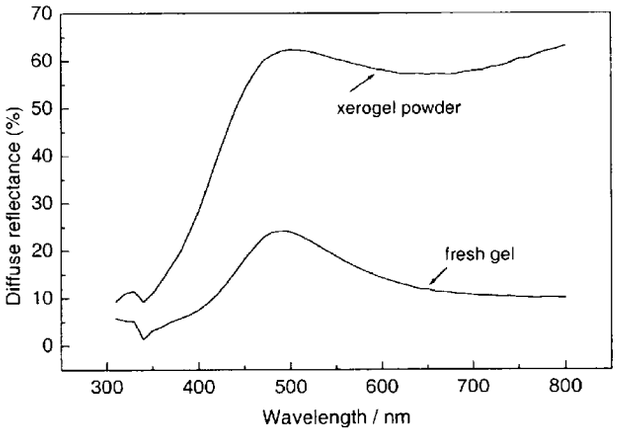

Fig. 2 Diffuse reflectance spectra of Mo–Ti oxide fresh gel and air-dried powder samples containing 70% Mo.

obtained from precursor solutions with Mo contents greater than 40% gradually turned blue after exposure to ambient light. The resultant xerogel powders also had a bluish tinge. Fig. 2 shows the diffuse reflectance spectra of the fresh gel and air-dried powder with 70% Mo. Wide absorption bands can be seen in the red–yellow light region, which causes the blue colour: the fresh gel was much bluer than the powder.

To find out the reason for the photo-colouration of Mo–Ti oxide gel, XPS was used to examine the chemical states and composition of the xerogel powder with the blue tinge (70% Mo). Fig. 3 shows the wide-scan XPS spectrum of the Mo–Ti oxide powder. Peaks corresponding to each of the elements can be seen from the figure; the powder contains Mo, Ti, O and C near its surface. In the insert, it can be seen that very weak peaks accompany the C 1s main peak to both higher and lower energies, which could be ascribed to carbons in C–O and C–C, respectively, from residual n-butyl alcohol adsorbed on the particle surface.

The bonding states of the Mo–Ti oxide powder were investigated using Mo 3d, Ti 2p and O 1s peaks, as shown in Fig. 4–6 with both raw and fitted data. It can be seen from Fig. 4 and 5 that only one electronic state of Mo or Ti exists in the detectable surface region. The photoelectron peaks at 232.7 and 458.6 eV are in agreement with literature values for Mo(VI) $3d_{5/2}$ and Ti(IV) $2p_{3/2}$, respectively.[12–14]

The O 1s line with $E_b = 530.5$ eV (P_2) can be assigned to the lattice oxygen of the MoO_3 and TiO_2 oxides. The second O 1s line with $E_b = 532.6$ eV (P_1) can be assigned to mixed contributions from surface hydroxide, peroxide and C–O.[13]

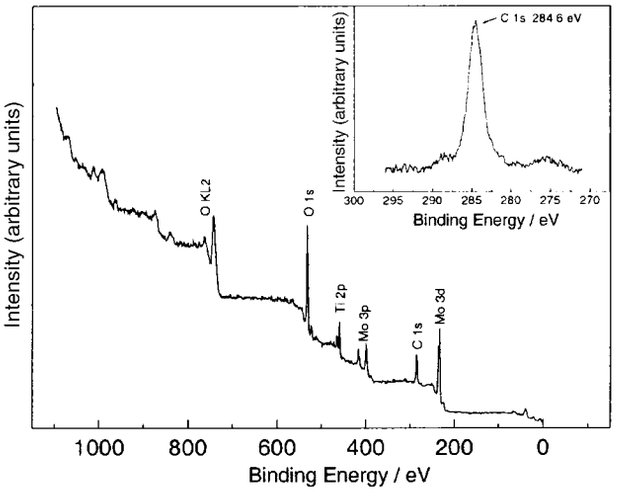

Fig. 3 XPS survey of the surface of Mo–Ti oxide powder containing 70% Mo. The insert shows the C 1s core level.

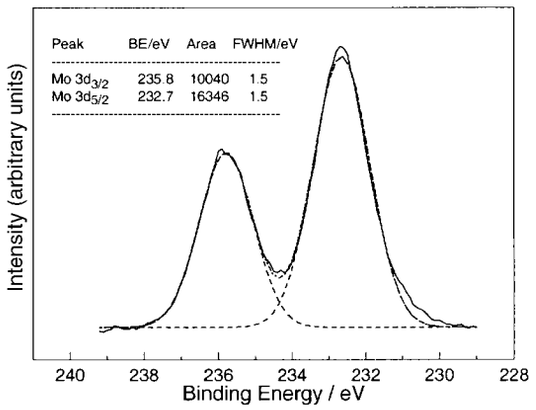

Fig. 4 Mo 3d XPS peak of Mo–Ti oxide powder containing 70% Mo.

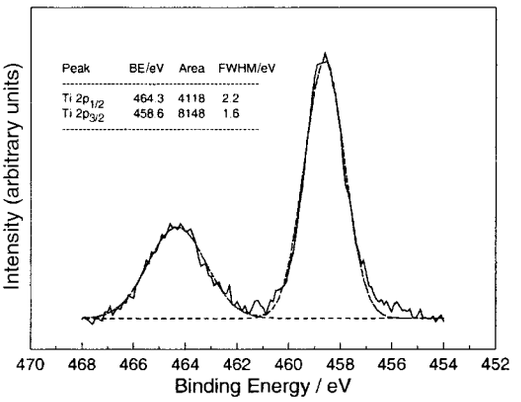

Fig. 5 Ti 2p XPS peak of Mo–Ti oxide powder containing 70% Mo.

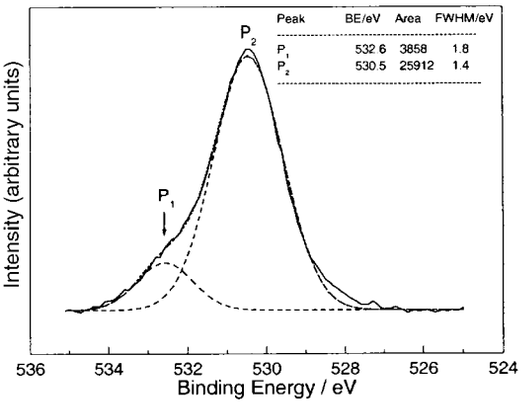

Fig. 6 O 1s XPS peak of Mo–Ti oxide powder containing 70% Mo.

Based on the above XPS results, we explain the photocolouration of the Mo–Ti oxide gels as follows.

Tennakone *et al.*[15] found that hydrated tungsten oxide $WO_3{\cdot}xH_2O$ in contact with TiO_2 grains suspended in water was reduced to $WO_{2.96}{\cdot}xH_2O$ upon irradiation with UV light. By measuring the band position of $WO_3{\cdot}xH_2O$, they found that the relative positions of the valence band and conduction band of WO_3 are lower than those of TiO_2, and suggested that electron transfer from TiO_2 to $WO_3{\cdot}xH_2O$ is responsible for the reduction. Considering the similarity of WO_3 and MoO_3, we assume that the relative positions of the valence band and conduction band of MoO_3 are also lower than those of TiO_2, and so a heterojunction is formed between MoO_3 and TiO_2.

When the gel is irradiated with visible light, the electrons in the valence band of the MoO_3 grains are excited to the conduction band, leaving holes in the valence band. (As an example, recently, Li and El-Shall[16] observed a considerable photochromic effect under ambient light for MoO_3 nanoparticles prepared by a laser vaporisation-controlled condensation technique.) As a consequence, electrons in the valence bands of TiO_2 are injected into the MoO_3 grains (while photogenerated holes move into the valence band of TiO_2 in the opposite direction) driven by the built-in field in the TiO_2–MoO_3 heterojunction. At the same time, this also intensifies the electron transition of MoO_3.

$$MoO_3 + h\nu \rightarrow MoO_3 + h^+(vb) + e^-(cb) \quad (2)$$

Holes can then oxidise adsorbed surface species, such as water or organic residue, forming protons which then migrate into MoO_3 grains through diffusion or Coulombic attraction. In our case of fresh gel or xerogel powder, both water and organic residue exist as adsorbents on the surface of MoO_3–TiO_2 coupled particles. The product of the hydrolysis reaction of $Ti(OBu^n)_4$ is Bu^nOH, so it is reasonable to assume that this is the organic residue, an alcohol with α-H which can easily be oxidised into an aldehyde. For example, it has been reported that organic additives containing O–C–H bonds in their chemical structures can improve the photochromism of tungstic acid remarkably.[17]

$$H_2O + h^+ \rightarrow {}^{\cdot}OH + H^+ \quad (3)$$

$$-CH_2-OH + h^+ \rightarrow -CHO + H^{\cdot} + H^+ \quad (4)$$

$$H^{\cdot} + {}^{\cdot}OH \rightarrow H_2O \quad (5)$$

Electrons in the conduction band react with the protons, resulting in a photo-intercalation process very similar to that described in reaction 1, and colour centres near the surface of the MoO_3 particles are created.[18]

$$MoO_3 + yH^+ + ye^- \rightarrow H_yMoO_3 \quad (6)$$

When the light blue powder was placed in the UHV analysis chamber of the XPS system, most of the physisorbed water and organic residue would have been desorbed. Since these are essential to the colouration process, no new colour centres could be formed after the existing ones had decomposed, which is expected to take place very quickly under UHV. As a matter of fact, we found that the powder had turned yellow–brown after it was removed from the chamber. Therefore, we were unable to find any reduced chemical states for either Ti or Mo from the XPS spectra.

Electrochromic properties of Mo–Ti oxide films

Cyclic voltammetry experiments were performed in the potential range between −1 and +1 V (starting from 0 V) and at a scanning rate of 20 mV s^{-1}. The electrochromic properties of the Mo–Ti oxide films were investigated by *in situ* monochromatic transmittance measurements when Li^+/e^-

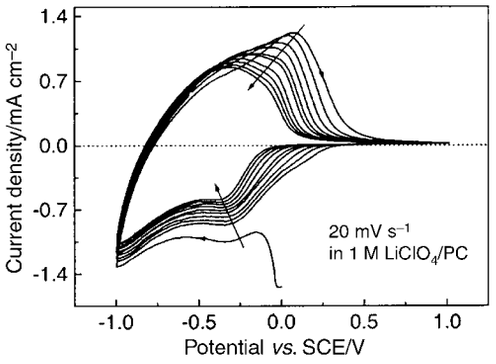

Fig. 7 Cyclic voltammogram of Mo–Ti oxide film. The arrows on the curve indicate the potential scan directions, while the other two indicate the movement of the cathodic/anodic waves.

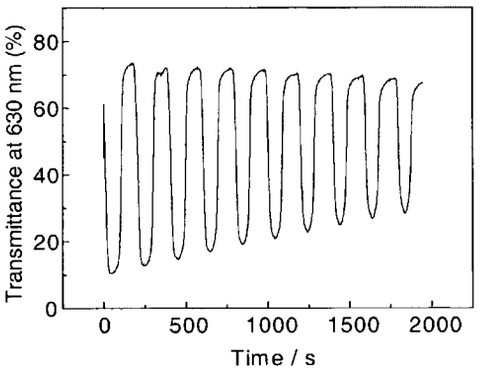

Fig. 8 Change in transmittance for the first 10 CV cycles in Fig. 7.

were intercalated into the oxide matrix during the CV process, taking the electrochemical cell with electrolyte as the reference. Data were recorded during the first 10 cycles, as shown in Fig. 7 and 8.

The shape of the voltammogram is typical for amorphous WO_3 or MoO_3 films.[3] Current response diminished with cycling (Fig. 7) and, correspondingly, the optical modulation range at 630 nm also evolved during cycling (Fig. 8). However, after 10 cycles training, the CV was stabilised, and no obvious change was observed, even after 1000 cycles. In comparison with data for pure MoO_3 films in the literature,[19] it is obvious that the addition of Ti has a stabilising effect on the charge capacity, which is essential for a device designed for long-term operation.

In Fig. 9, the optical densities (OD) are plotted against the charge density (Q), where the charge density was calculated by integrating the current response in Fig. 7, and the optical density was calculated from the transmittance in Fig. 8 according to $OD = -\log T$. From the slope of the linear section, a colouration efficiency at 630 nm of 30.6 $cm^2\,C^{-1}$ is obtained, which is lower than the value of 50 $cm^2\,C^{-1}$ found for pure MoO_3 films,[7] but high enough for practical applications. One notable feature occurs at the beginning of charge insertion, where a delay or retrogression of the OD increase takes place. This phenomenon was also observed in our previous work for peroxo sol–gel derived TiO_2 films,[10] and can be similarly explained as the oxidisation of 'molybdenum bronze' by the peroxo remnants left in the as-deposited film.

Fig. 10 shows *ex situ* optical transmittance data for the Mo–Ti oxide film in the as-deposited state, and after polarisation at -1 and $+1$ V for 60 s, for the coloured and bleached states, respectively. The Li^+ intercalated film was dark grey while the deintercalated film was transparent. The transmittance change (ΔT) for the film between the bleached and coloured states was larger than 30% for nearly the whole visible light region and the film always displayed a neutral colour.

Fig. 11 shows the transmittance of the coloured Mo–Ti oxide

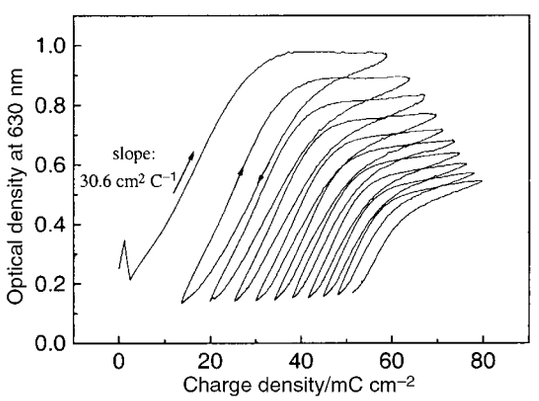

Fig. 9 Change in optical density at 630 nm as a function of charge density for the first 10 CV cycles in Fig. 7.

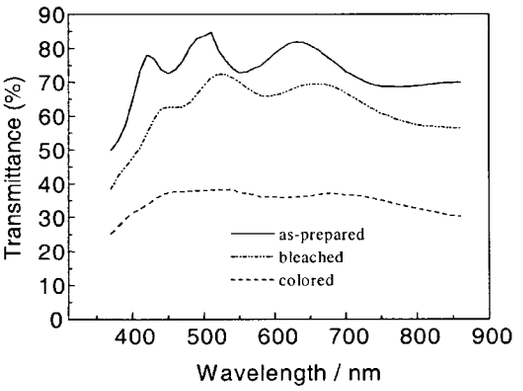

Fig. 10 Transmittance spectra of Mo–Ti oxide film in different states.

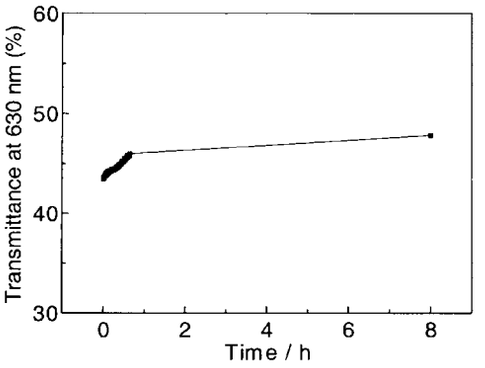

Fig. 11 Transmittance at 630 nm of the coloured Mo–Ti oxide film as a function of time in air. Data were recorded for the starting period and end point of exposure.

film as a function of time of exposure in air. After 8 h only a slight increase in transmittance was observed especially in the early stage when the film was exposed to air. This result indicates that the 'molybdenum bronze' is very stable towards air oxidation. In contrast, we observed severe self-bleaching behaviour when sol–gel-derived WO_3 films in the coloured state were exposed to air.[20]

4 Conclusion

The following can be concluded: (i) a simple aqueous sol–gel route to prepare Mo–Ti mixed oxide gels, powders or thin films using H_2O_2 as a chelating agent has been demonstrated. (ii) The Mo–Ti oxide gel with $>40\%$ Mo became blue under ambient light irradiation. It is proposed that TiO_2 particles and surface species, including adsorbed water and organic residue, all play important roles in the photochromic effect of MoO_3. (iii) The Mo–Ti mixed oxide films showed excellent electrochromic properties.

Acknowledgements

The financial support from the National Climbing Program of China (Grant No. 07-01) and the National Natural Science Foundation of China (Grant Nos. 59782006 and 59932040) is gratefully acknowledged.

References

1 J. G. H. Mathew, S. P. Sapers, M. J. Cumbo, R. B. Sargent, N. A. O'Brien, V. P. Raksha, R. B. Lahaderne and B. P. Hichwa, *J. Non-Cryst. Solids*, 1997, **218**, 342.
2 N. A. O'Brien, J. G. H. Mathew and B. P. Hichwa, *Thin Solid Films*, 1999, **345**, 312.
3 C. G. Granqvist, *Handbook of Inorganic Electrochromic Materials*, Elsevier, Amsterdam, 1995.

4 O. Zelaya-Angel, C. Menezes, F. Sahnches-Sinencio and G. F. L. Ferreira, *J. Appl. Phys.*, 1980, **51**, 6022.
5 S. Doeff and C. Sanchez, *C. R. Acad. Sci., Ser. II*, 1989, **309**, 531.
6 Z. Wang, X. Chen and X. Hu, *Proc. SPIE-Int. Soc. Opt. Eng.*, 1997, **3175**, 247.
7 L. Kullman, A. Azens and C. G. Granqvist, *Sol. Energy Mater. Sol. Cells*, 2000, **61**, 189.
8 S. Sato and Y. Seino, *Trans. Inst. Electron. Commun. Eng. Jpn. Sect. C*, 1982, **65**, 629.
9 Y.-M. Li and T. Kudo, *Sol. Energy Mater. Sol. Cells*, 1995, **39**, 179.
10 Z. Wang and X. Hu, *Thin Solid Films*, 1999, **347**, 62.
11 L. H. Dao, A. Guerfi and M. T. Nguyen, *Proc. Electrochem. Soc.*, 1990, **90–92**, 30.
12 I. Nova, L. Lietti, L. Casagrande, L. Dall'Acqua, E. Giamello and P. Forzatti, *Appl. Catal., B*, 1998, **17**, 245.
13 J. F. Moulder, W. F. Stickle, P. E. Sobol and D. Bomben, *Handbook of X-ray photoelectron spectroscopy*, Physical Electronics Inc., Eden Prairie, MN, 1995.
14 Y. L. Leung, P. C. Wong, K. A. R. Mitchell and K. J. Smith, *Appl. Surf. Sci.*, 1998, **136**, 147.
15 K. Tennakone, O. A. Ileperuma, J. M. S. Bandara and W. C. B. Kiridena, *Semicond. Sci. Technol.*, 1992, **7**, 423.
16 S. Li and M. S. El-Shall, *Nanostruct. Mater.*, 1999, **12**, 215.
17 K. Kuboyama, K. Hara, K. Matsushige1 and S. Kai, *Jpn. J. Appl. Phys., Part 2*, 1997, **36**, L443.
18 S. K. Deb and J. A. Chopporian, *J. Appl. Phys.*, 1966, **37**, 4818.
19 A. Guerfi, R. W. Paynter and L. H. Dao, *J. Electrochem. Soc.*, 1995, **142**, 3457.
20 Z. Wang, Ph D thesis, Shanghai Institute of Ceramics, Chinese Academy of Sciences, 1998.